

## Novel Visible-Light-Driven Photocatalyst. Poly(*p*-phenylene)-Catalyzed Photoreductions of Water, Carbonyl Compounds, and Olefins

Takuya Shibata, Akira Kabumoto, Tsutomu Shiragami, Osamu Ishitani, Chyongjin Pac, and Shozo Yanagida\*

Chemical Process Engineering, Faculty of Engineering, Osaka University, Suita, Osaka 565, Japan  
(Received: August 8, 1989)

The insoluble yellow powder of poly(*p*-phenylene) (PPP) prepared by nickel-catalyzed polycondensation of the Grignard reagent from 1,4-dibromobenzene shows photocatalytic activity under visible light toward water, carbonyl compounds, and olefins. Water is photoreduced to H<sub>2</sub> in the presence of amines as sacrificial electron donors. The H<sub>2</sub> evolution is enhanced 3–20 times by noble-metal deposition, in which Ru deposition is the most effective. Apparent quantum yields ( $\Phi(^{1/2}\text{H}_2)$ ) for Ru-loaded PPP-catalyzed H<sub>2</sub> evolution depend on the irradiation wavelength, reaching a maximum value of 0.015 at 405 nm. On the other hand, nonmetallized PPP can more efficiently photocatalyze the reduction of carbonyls and electron-deficient olefins by triethylamine in methanol compared to Ru-loaded PPP, in cases where the reduction potentials of the substrates are more positive than –2.0 V vs Ag/0.01 M AgNO<sub>3</sub>. The carbonyls are reduced to the corresponding alcohols and/or pinacols, whereas the reduction of the olefins to the dihydro compounds is accompanied by rapid *cis*–*trans* photoisomerization. From the deuterium incorporation experiments for the photocatalyzed reduction of methyl 4-cyanocinnamate, **6j**, in methanol-*O-d*, disproportionation of one-electron-transfer reduction intermediates is suggested to be responsible for the eventual two-electron reductions and the *cis*–*trans* photoisomerization. The physical and spectral properties of PPP's are characterized, and the mechanism is discussed in terms of the energy structure.

Since the photolysis of water on a TiO<sub>2</sub> electrode (Honda–Fujishima effect) was reported,<sup>1</sup> photoinduced charge separation on inorganic semiconductors has been widely investigated as a key step in the conversion of light to chemical potential energy.<sup>2</sup> In order to achieve high efficiency in photochemical conversion or to utilize visible light much more effectively, integrated chemical systems using semiconductor/redox couple interfaces combined with metallic cocatalysts, electron relays, sensitizers, or polymers have been extensively studied.<sup>2,3</sup>

On the other hand, since polyacetylene film was synthesized and chemical doping effects on electric conductivity were discovered,<sup>4</sup> a number of organic polymers with conjugated  $\pi$ -electrons have been synthesized and some novel applications such as electrochromic polymers,<sup>5</sup> organic batteries,<sup>6</sup> sensing polymers,<sup>7</sup> and solar batteries<sup>8</sup> have been successfully proposed. Conjugated polymers called conducting polymers show electrical conductivity only when they are doped chemically with either electron donors or acceptors. Under undoped conditions, however, they are semiconducting and should be called polymeric organic semiconductors.<sup>9</sup> Among such  $\pi$ -bond conjugated polymers, poly(*p*-phenylene) (PPP) polymers are resistant to oxidation, thermal degradation, and radiation under aerobic conditions<sup>10</sup> and are reported to have band gaps in the visible-light region.<sup>11</sup> Evolution

of the polymer's electronic properties is explained in terms of the chain geometry in PPP, which, on doping, relaxes toward the quinoidlike resonance structure that has a lower ionization potential and a larger electronic affinity and thus yields static electronic carriers.<sup>9,12</sup> Such a mechanism suggests that, upon photoexcitation, some parts of PPP chains that may be subject to the quinoidlike structure might give rise to intra- or intermolecular charge-separated states in the solid PPP assembly. From these points of view, we expected photocatalytic activity in photostable PPP powder. Previously, we reported initial photocatalysis of PPP for water photoreduction under UV-light irradiation<sup>13</sup> and for *cis*–*trans* photoisomerization of simple olefins under visible light.<sup>14</sup> In this paper, we present results of a complete study of PPP characterization and its photocatalysis, showing that PPP interfaces provide an effective system for charge separation leading to water photoreduction in aqueous medium and photoreductions of unsaturated compounds in nonaqueous medium under visible-light irradiation.

### Results

#### Preparation and Chemical Structure of PPP Photocatalyst.

A number of different procedures have been used for the preparation of PPP. For the present study on catalysis, PPP powder was prepared according to Yamamoto's method,<sup>15</sup> i.e., by polymerization of the Grignard reagent obtained from 4,4'-dibromobiphenyl or 1,4-dibromobenzene. The PPP prepared from the former bromide contains a higher bromine content than that from the latter. Since both PPP's are insoluble even in hot toluene (see Experimental Section), it was difficult to characterize their structure.<sup>15,16</sup> According to the recent report on the molecular weight distribution and end-group composition of PPP based on a newly developed mass spectral analysis (LD/FT-mass),<sup>17</sup>

- (1) Fujishima, A.; Honda, K. *Nature* **1972**, *238*, 37.
- (2) (a) Bard, A. J. *J. Phys. Chem.* **1982**, *86*, 172. (b) Grätzel, M. *Energy Resources through Photochemistry and Catalysis*; Academic Press: New York, 1983. (c) Kalyanasundram, K.; Grätzel, M. *Photochem. Photobiol.* **1984**, *40*, 807.
- (3) (a) Kakuta, N.; Park, K.-H.; Finlayson, M. F.; Bard, A. J.; Campion, A. A.; Fox, M. A.; Webber, S. E.; White, J. M. *J. Phys. Chem.* **1985**, *89*, 5028. (b) Bard, A. J. *Ber. Bunsen-Ges. Phys. Chem.* **1988**, *92*, 1187.
- (4) Chiang, C. K.; Fincher, C. R., Jr.; Park, Y. W.; Heeger, A. J.; Shirakawa, H.; Louis, E. J.; Gau, S. C.; MacDiarmid, A. G. *Phys. Rev. Lett.* **1977**, *39*, 1098.
- (5) (a) Yoshino, K.; Kaneto, K.; Inuishi, Y. *Jpn. J. Appl. Phys.* **1983**, *22*, L157. (b) Osawa, J.; Kaneto, K.; Yoshino, K. *Jpn. J. Appl. Phys.* **1984**, *23*, L527.
- (6) (a) Nigrey, P. J.; MacInnes, D.; Nairns, D. P.; MacDiarmid, A. G.; Heeger, A. J. *J. Electrochem. Soc.* **1981**, *128*, 1651. (b) Shacklette, L. W.; Elsenbaumer, R. L.; Chance, R. R.; Sowa, J. M.; Ivory, D. W.; Miller, G. G.; Baughman, R. H. *J. Chem. Soc., Chem. Commun.* **1982**, 361.
- (7) (a) Yoshino, K.; Hayashi, S.; Kohno, Y.; Kaneto, K.; Okube, J.; Moriya, T. *Jpn. J. Appl. Phys.* **1984**, *23*, L198. (b) Dong, S.; Sun, Z.; Lu, Z. *J. Chem. Soc., Chem. Commun.* **1988**, 993.
- (8) Tani, T.; Grant, P. M.; Gill, W. D.; Street, G. B.; Clark, T. C. *Solid State Commun.* **1980**, *33*, 499.
- (9) Brédas, J. L.; Street, G. B. *Acc. Chem. Res.* **1985**, *18*, 309.
- (10) Kovacic, P.; Jones, M. B. *Chem. Rev.* **1987**, *87*, 357.

- (11) (a) Brédas, J. L.; Chance, R. R.; Baughman, R. H. *J. Chem. Phys.* **1982**, *76*, 3673. (b) Brédas, J. L.; Silbey, R.; Boudreaux, D. S.; Chance, R. R. *J. Am. Chem. Soc.* **1983**, *105*, 6555. (c) Seki, K.; Karlsson, U. O.; Engelhardt, R.; Koch, E.-E.; Schmidt, W. *Chem. Phys.* **1984**, *91*, 459. (d) Tabata, M.; Satoh, M.; Kaneto, K.; Yoshino, K. *J. Phys. C: Solid State Phys.* **1986**, *19*, L101.
- (12) Chance, R. R.; Brédas, J. L.; Silbey, R. *Phys. Rev. B.* **1984**, *29*, 4491.
- (13) Yanagida, S.; Kabumoto, A.; Mizumoto, K.; Pac, C.; Yoshino, K. *J. Chem. Soc., Chem. Commun.* **1985**, 474.
- (14) Yanagida, S.; Hanazawa, M.; Kabumoto, A.; Pac, C.; Yoshino, K. *Synth. Met.* **1987**, *18*, 785.
- (15) (a) Yamamoto, T.; Yamamoto, A. *Chem. Lett.* **1977**, 353. (b) Yamamoto, T.; Hayashi, Y.; Yamamoto, A. *Bull. Chem. Soc. Jpn.* **1978**, *51*, 2091.
- (16) Sato, M.; Kaeriyama, K. *Makromol. Chem.* **1983**, *184*, 2241.

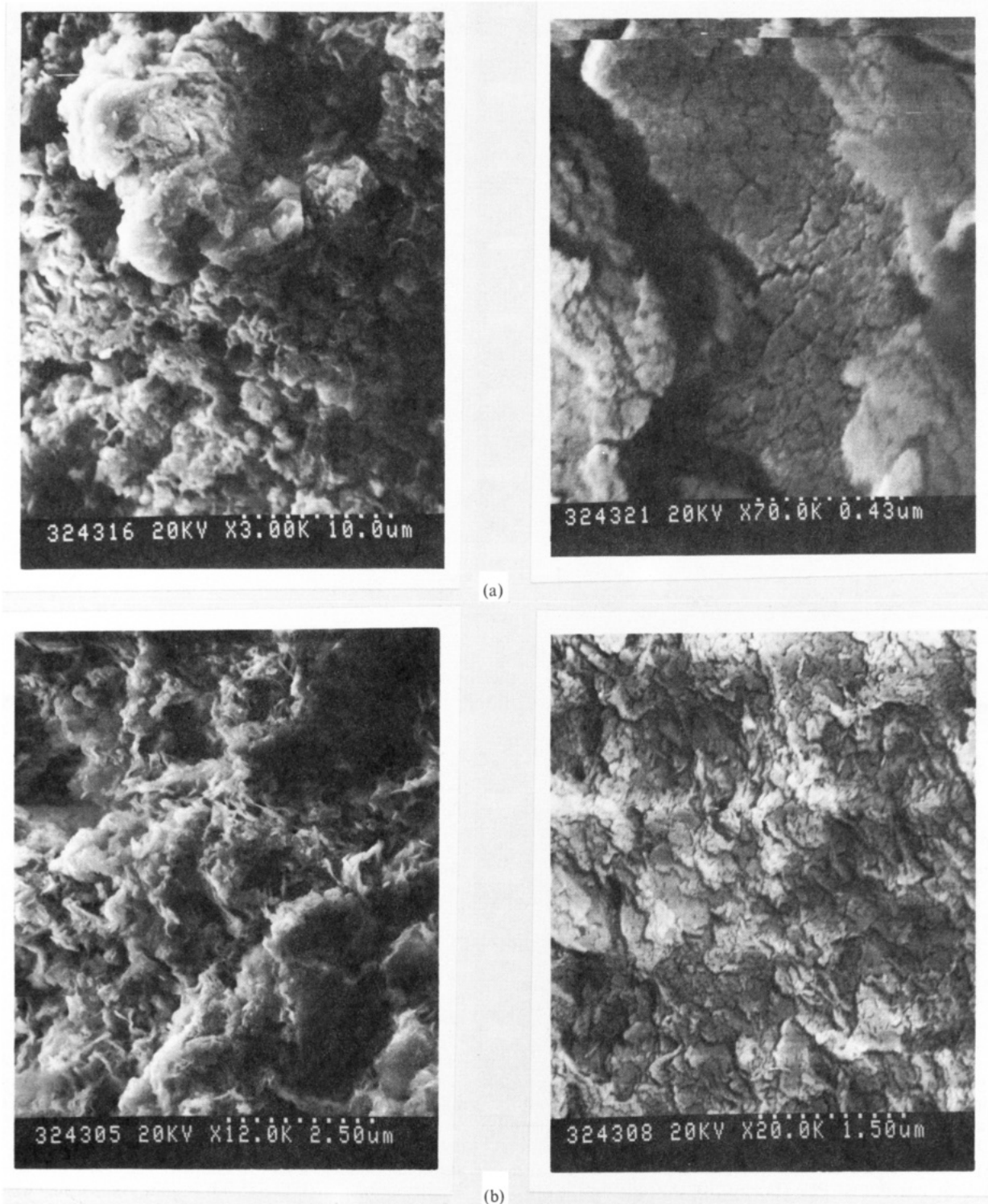


Figure 1. Scanning electron micrographs: (a) PPP-7; (b) PPP-11.

Yamamoto's PPP of a 6.2% bromine content was characterized to be a mixture of bromine-free PPP (4–25 benzene rings) and PPP terminated with one 4-bromophenyl group. Calculations show an average chain length of 13–14 *p*-phenylene rings. Therefore, we presumed that the two kinds of PPP prepared consist of a similar mixture of PPP's with a linear sequence of *p*-phenylene rings containing no or only one bromine atom at one end. On the basis of bromine analysis and the comparison with the reported LD/FT-mass data, the average number of *p*-phenylene rings was estimated to be 6.5 and 11, respectively, for the high-bromine-containing PPP (14.14% Br) and the lower one (8.37% Br), and

they were termed PPP-7 and PPP-11, respectively.

**Physical Properties of PPP's.** Scanning electron micrographs (Figure 1) show that both PPP's have a feathery and porous structure and there is no significant difference in their appearance. The specific surface areas of PPP-7 and PPP-11 were determined by the BET method to be 39 and 44 m<sup>2</sup>/g, respectively. The densities of PPP-7 and PPP-11 were determined by flotation to be 1.51 and 1.40 g/cm<sup>3</sup>, respectively. Taking into account their bromine contents and the densities of *p*-terphenyl (1.27 g/cm<sup>3</sup>) and *p*-sexiphenyl (1.34 g/cm<sup>3</sup>), they were characterized to have fairly low densities. In fact, both PPP's are dispersed in methanol with good stability after sonication.

**Spectral Characteristics of PPP Photocatalysts.** The absorption spectra of suspensions of PPP-11 and PPP-7 in methanol are shown

(17) Brown, C. E.; Kovacic, P.; Wilkie, C. A.; Cody, R. O., Jr.; Kinsinger, J. A. *J. Polym. Sci., Polym. Lett. Ed.* **1985**, *23*, 453.

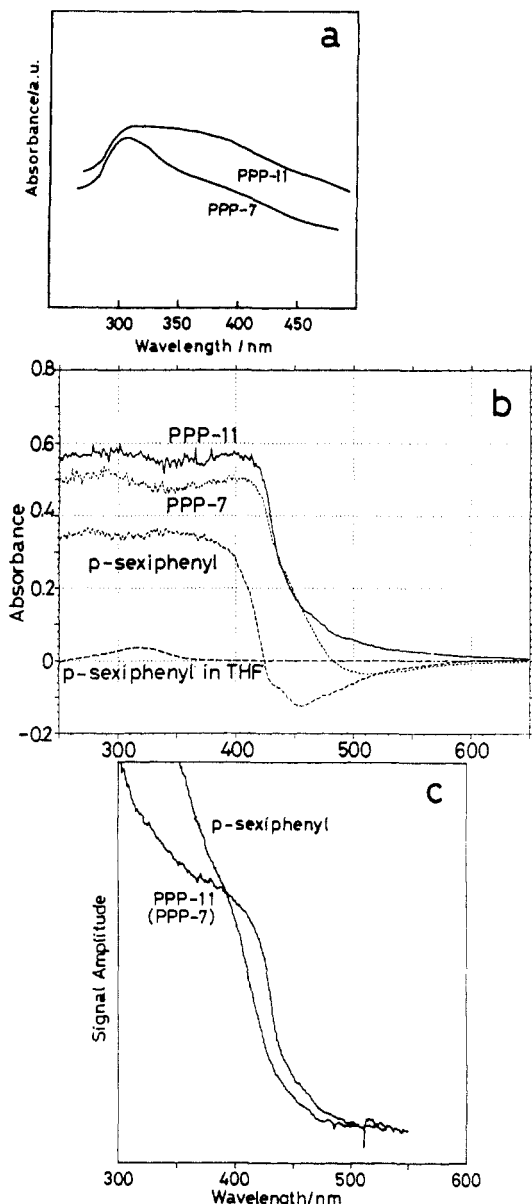


**Figure 2.** (a) Absorption spectra of PPP catalysts suspended in methanol. (b) Absorption spectra of PPP catalysts and *p*-sexiphenyl by reflectance spectrometry using a Photal. (c) Photoacoustic spectra of PPP-11 and *p*-sexiphenyl.

in Figure 2a. Compared with PPP-7, PPP-11 has an absorption ranging to longer wavelengths. This difference is consistent with the fact that PPP-11 has a longer chain length of *p*-phenylene than PPP-7. However, their absorption spectra in the solid state, measured by reflectance spectrometry using a multichannel photodiode system (MCPD) (Figure 2b), were almost the same except for the emissive pattern around 500 nm of PPP-7.<sup>18</sup> The photoacoustic spectrum of PPP-11 (Figure 2c) was also identical with that of PPP-7 and reveals a sharp rise around 460 nm as shown in Figure 2b. For comparison, the absorption spectra of *p*-sexiphenyl, a model compound of PPP, were also measured in the solid state by reflectance (MCPD) and photoacoustic spectrometry. Compared with the absorption spectrum of its saturated THF solution in Figure 2b, the onset of the absorption spectra in the solid state shifted to a longer wavelength, suggesting that the conjugation of phenylene units should increase much more

(18) In reflectance MCPD spectra of Figure 2b, characteristic emissions are seen around 500 nm for PPP-7 and 450 nm for *p*-sexiphenyl. No emission in PPP-11 may be due to the quenching of the emission by longer *p*-phenylene derivatives included in PPP-11 in the MCPD spectrometry. The overlap of the absorption and emission spectra of PPP-11 in Figure 3 also supports this explanation.

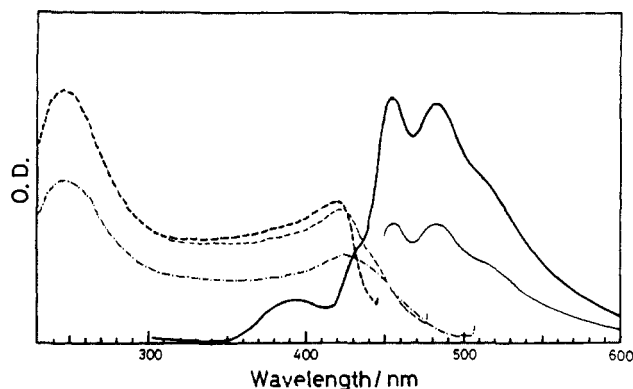


**Figure 3.** Photoluminescence spectra of PPP-11 and excitation spectra of PPP-11: (bold solid line) excited at 250 nm; (light solid line) excited at 420 nm; (bold dashed line) monitored at 455 nm; (light dashed line) monitored at 485 nm; (dot-dash line) monitored at 515 nm.

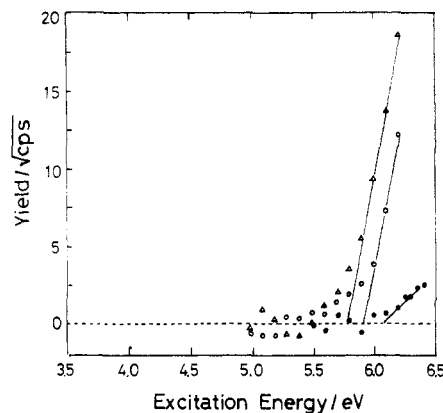


**Figure 4.** AUP spectra of PPP-7, PPP-11, and *p*-sexiphenyl: ( $\Delta$ ) *p*-sexiphenyl; ( $\circ$ ) PPP-7; ( $\bullet$ ) PPP-11 (The gentle slope is due to the low intensity of incident light.)

in the solid state than in THF. Although the onset of the absorption spectrum of the solid *p*-sexiphenyl in Figure 2b is ambiguous due to strong emission around 450 nm,<sup>18</sup> the photoacoustic spectra (Figure 2c) clearly revealed the difference in the onset of the absorption spectra; also, the spectrum of PPP-11 (PPP-7) shifts to longer wavelength as much as ca. 15 nm more than that of *p*-sexiphenyl, supporting the idea that PPP's should consist of much longer *p*-phenylene units than that of *p*-sexiphenyl and the calculated average ones.

Figure 3 shows photoemission of PPP-11 powder in air and the excitation spectra monitored by the peak emissions at 455, 485, and 515 nm. The excitation spectra are different from each other and have a shift to a longer wavelength with an increase of the wavelength of the monitored light. These observations can be interpreted as being due to the excitation of PPP molecules having different chain lengths. In addition, the rise in the excitation spectrum monitored at 515 nm is quite comparable with those of the absorption spectra determined by the MCPD and photoacoustic spectrometry. Considering these spectral characteristics, the band gap ( $E_g$ ) was determined to be 2.90 eV (427 nm) for both PPP-7 and PPP-11, although they have a different distribution of the *p*-phenylene chain.

**Energy Structure of PPP's.** In order to evaluate the valence band structure of PPP photocatalysts, their ionization potentials (IP) were measured by an atmospheric ultraviolet photoelectron analyzer (AUP). AUP has recently been developed<sup>19</sup> and counts low energy electrons emitted from a solid surface in air, giving threshold energies for electron emission corresponding to the IP of organic semiconductors in the solid state. On the basis of AUP spectra (Figure 4), the IP's of PPP-7 and PPP-11 were determined to be 5.91 and 6.07 eV, respectively. *p*-Sexiphenylene, a good

(19) Kirihata, H.; Uda, M. *Rev. Sci. Instrum.* **1981**, *52*, 68.

TABLE I: Electronic Structure of PPP

| PPP    | IP/eV | $E_g$ /eV | $E_v^a$ /V | $E_c^b$ /V |
|--------|-------|-----------|------------|------------|
| PPP-7  | 5.91  | 2.90      | 0.87       | -2.03      |
| PPP-11 | 6.07  | 2.90      | 1.03       | -1.87      |

<sup>a</sup>  $E_v$ , upper edge of valence band (V) vs Ag/0.01 M AgNO<sub>3</sub>; calculated from  $E_v = IP - 5.04$ . <sup>b</sup>  $E_c$ , bottom of conduction band (V) vs Ag/0.01 M AgNO<sub>3</sub>; calculated from  $E_c = E_v - E_g$ .

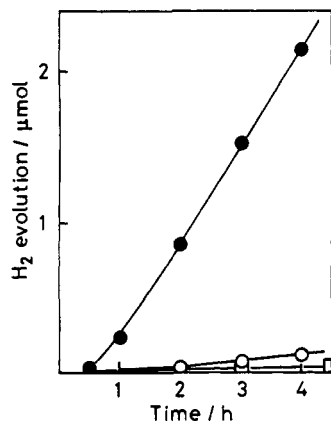


Figure 5. Water photoreductive H<sub>2</sub> evolution catalyzed by  $\pi$ -conjugated polymers: (●) PPP-11; (○) PPP-7; (□) poly(thiophene).

model compound for PPP, also gave a clear AUP spectrum under the same conditions, and its IP was determined to be 5.78 eV (Figure 4). This value agrees fairly well with the IP (5.9 eV) obtained from the threshold of its UPS spectrum.<sup>11</sup> It is unexpected, however, that the IP increases with increasing *p*-phenylene chain length, and PPP-11 has the largest IP. In order to make a quantitative comparison with redox reactions on irradiated PPP photocatalysts, the upper edge of the valence band and the bottom of the conduction band were evaluated in the electrochemical scale by assuming 5.04 eV<sup>11b</sup> as a scale factor relating Ag/0.01 M AgNO<sub>3</sub> to vacuum, and the results are summarized in Table I.

**Photoreduction of Water.** Figure 5 shows a comparison of the photocatalytic activity of some  $\pi$ -conjugated polymers for H<sub>2</sub> evolution from methanolic aqueous triethylamine (TEA) (1:1:1 v/v) under irradiation at >290 nm. PPP-11 was found to have a marked activity compared with PPP-7, indicating that the *p*-phenylene chain length plays an important role in the photocatalysis. However, dark-brown PPP powder prepared from benzene according to the Kovacic method<sup>20</sup> did not show photocatalytic activity under comparable conditions. In addition, polythiophene (PT) was also found quite inactive for the photocatalytic H<sub>2</sub> evolution, although PT showed the same catalytic activity for *cis*-*trans* photoisomerization of olefins as PPP.<sup>14</sup>

As reported in the previous paper,<sup>13</sup> PPP showed a slight activity for water reduction under visible light (>400 nm). To enhance the efficiency in the activity of PPP under visible light, some noble metals were photodeposited on PPP-11 with use of metal salt as the metal source and TEA as an electron donor under >290-nm irradiation (see Experimental Section). Surprisingly, the catalysis of PPP-11 was enhanced by metal photodeposition as shown in Figure 6. Especially, Ru-loaded PPP-11 (PPP-11-Ru) was more than twenty times as effective as unloaded PPP-11. However, contrary to TiO<sub>2</sub> photocatalysts,<sup>2,21</sup> the activity of PPP-11 was not enhanced when PPP-11 powder was treated only with Pt black or RuO<sub>2</sub> powder in a similar way as TiO<sub>2</sub> particles.

The source of hydrogen was confirmed to be water. The PPP-11 catalyzed photolysis in the presence of D<sub>2</sub>O generated D<sub>2</sub>, HD, and H<sub>2</sub> in a ratio of 65:9:1. The amount of D<sub>2</sub> increased much more compared with that obtained in the case of UV-irradiated

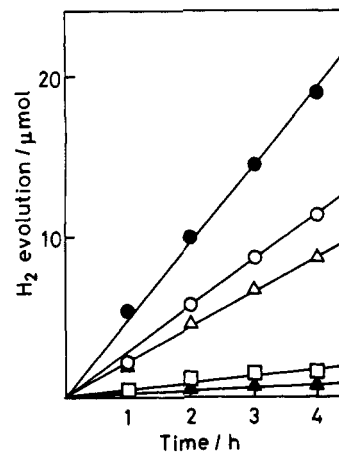


Figure 6. Effect of metal-loaded PPP-11 on H<sub>2</sub> photoevolution: (●) Ru-loaded; (○) Rh-loaded; (△) Pt-loaded; (□) Pd-loaded; (▲) none.

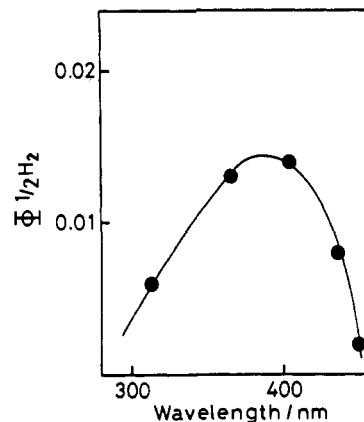


Figure 7. Action spectrum for photoevolution of H<sub>2</sub> catalyzed by PPP-11-Ru.

nonmetallized PPP-11.<sup>13</sup> This fact supports the idea that H<sub>2</sub> generation should be based on the more efficient photocatalysis of PPP-11-Ru.

Figure 7 shows an action spectrum of PPP-11-catalyzed H<sub>2</sub> evolution based on the quantum yields determined at definite wavelength. The quantum yields were all apparent ones, because they were not corrected for light absorption by the suspended catalysts. The maximum quantum yield was obtained approximately around the band-gap excitation (405 nm) and determined to be 0.015 by assuming that two photons produce one molecule of H<sub>2</sub>. It should be noted that the quantum yield decreased at wavelengths shorter than the band gap. To eliminate the contribution of a variation of the penetration depth of the light, the use of PPP, which was confirmed to be well dispersed under irradiation, was minimized in its concentration. Degradation of the catalyst never occurred under the irradiation conditions, and the dependence of H<sub>2</sub> evolution on the wavelength of light was confirmed by repeated experiments using the same reaction system. It seems that the action spectrum is fairly parallel to the excitation spectra (Figure 3), which shows a slight decrease in the range between 300 and 400 nm. However, further work is required to give a satisfactory explanation for the sharp drop in quantum yield around 300 nm.

**Sacrificial Electron Donors for PPP-Photocatalyzed H<sub>2</sub> Evolution.** In Table II are summarized the quantities of H<sub>2</sub> evolved by irradiation of various amines in aqueous methanol in the presence of PPP-11 or PPP-11-Ru. Most amines whose oxidation potentials are around 1.0 V vs Ag/0.01 M AgNO<sub>3</sub> work as a sacrificial electron donor for the water photoreduction. However, ammonia and benzylamine were poor electron donors and *tert*-butylamine did not work as an electron donor. Ascorbic acid ( $E_p = 0.02$ ) and EDTA-Na salt ( $E_{1/2} = 1.07/W$ ) were poor electron donors for this novel system possibly because of their hydrophilic properties. When Ru was photodeposited on PPP-11. TEA and

(20) Kovacic, P.; Kyriakis, A. *J. Am. Chem. Soc.* **1963**, *85*, 454.

(21) Mills, A.; Porter, G. *J. Chem. Soc., Faraday Trans. 1* **1982**, *78*, 3659.

(22) *CRC Handbook Series in Organic Electrochemistry*; Meites, L., Zuman, F., Eds.; CRC Press: Cleveland, OH, 1976; Vol. 1.

**TABLE II: PPP-Catalyzed Photoreduction of Water to H<sub>2</sub> in the Presence of Various Sacrificial Electron Donors**

| electron donor             | $E_{1/2}^{ox}/V$                     | H <sub>2</sub> evolution/<br>( $\mu\text{mol}/4\text{ h}$ ) |                  |
|----------------------------|--------------------------------------|-------------------------------------------------------------|------------------|
|                            |                                      | PPP-11                                                      | PPP-11-Ru        |
|                            |                                      | >290 nm <sup>c</sup>                                        |                  |
| hydrazine                  | -0.22/W <sup>b</sup>                 | 1.4                                                         | 24               |
| triethylamine              | 0.66 (0.69/W ( $E_p$ )) <sup>b</sup> | 2.5                                                         | 22               |
| tri- <i>n</i> -propylamine | 0.64                                 | 1.1                                                         | 4.8 <sup>d</sup> |
| trimethylamine             | 0.82 (0.76/W) <sup>b</sup>           | 1.1                                                         | 6.5              |
| di- <i>n</i> -propylamine  | 0.90/W ( $E_p$ ) <sup>b</sup>        | 0.5                                                         | 2.7              |
| diethylamine               | 1.01                                 | 0.7                                                         | 3.6              |
| dimethylamine              | 1.03/W ( $E_p$ ) <sup>b</sup>        | 1.0                                                         | 1.2              |
| <i>n</i> -propylamine      | 1.13                                 | 1.3                                                         | 2.0              |
| <i>n</i> -butylamine       | 1.13                                 | 1.1                                                         | 2.2              |
| benzylamine                |                                      | 0.02                                                        | 1.1              |
| ammonia                    |                                      | 0.02                                                        | 0.1              |
| <i>tert</i> -butylamine    |                                      | 0                                                           | 0                |
|                            |                                      | >400 nm <sup>e</sup>                                        |                  |
| triethylamine              | 0.66                                 | 0.4                                                         | 1.1              |
| DMB <sup>f</sup>           | 0.71                                 | trace                                                       | 1.7              |
| DMT <sup>g</sup>           | 0.7 ( $E_p$ ) <sup>b</sup>           | 0.4                                                         | 0.6              |

<sup>a</sup> Polarographic half-wave oxidation potentials vs Ag/0.01 M AgNO<sub>3</sub> in CH<sub>3</sub>CN. See ref 22. <sup>b</sup> See ref 22: vs SCE,  $E_p$ ; peak potential, W; in H<sub>2</sub>O. <sup>c</sup> Conditions: donor, 0.5 mL; CH<sub>3</sub>OH, 0.5 mL; H<sub>2</sub>O, 0.5 mL. <sup>d</sup> Conditions: donor, 0.5 mL; H<sub>2</sub>O, 0.1 mL, CH<sub>3</sub>OH, 0.9 mL. <sup>e</sup> Conditions: donor, 1 M; H<sub>2</sub>O, 0.5 mL; CH<sub>3</sub>OH, 0.5 mL. <sup>f</sup> *N,N*-Dimethylbenzylamine. <sup>g</sup> *N,N*-Dimethyltoluidine.

hydrazine became excellent sacrificial electron donors for the water photoreduction.

As photoproducts from TEA in the PPP-11-Ru system, diethylamine (DEA) was formed concurrently with H<sub>2</sub>. In addition, ethanol was also detected as another reduction product as shown in Figure 8. Acetaldehyde was also detected but not monitored because it is unstable in alkaline reaction solutions. The formation of DEA and acetaldehyde can be explained by hydrolysis of the two-electron oxidation product (1) of TEA.

Assuming electron and hole pairs are formed on irradiated PPP, the observed photoreactions in aqueous PPP/TEA system can be depicted as Scheme I.

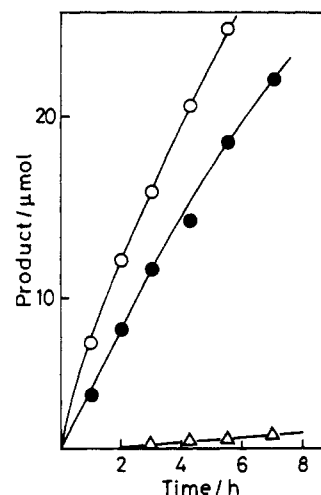
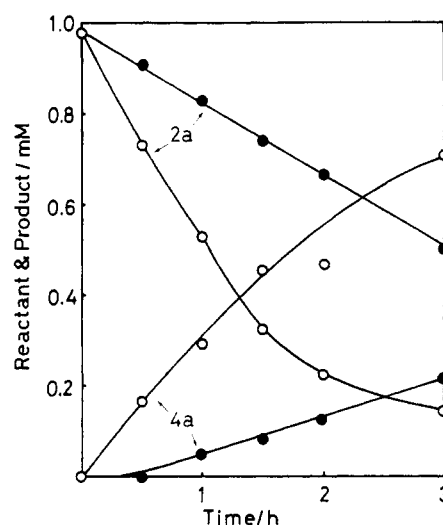
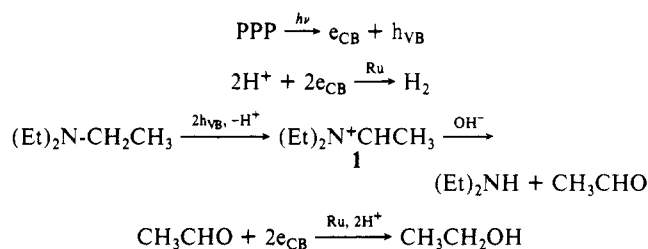
**Photoreduction of Carbonyl Compounds.** The PPP-catalyzed photosystem has been successfully extended to reduction of some carbonyl compounds **2** in methanol with use of TEA as an electron donor. Figure 9 presents time-conversion plots for the photoreduction of methyl benzoylformate (MBF, **2a**) catalyzed by PPP-11 and PPP-11-Ru under visible-light (>400-nm) irradiation. The reduction of MBF was more efficiently achieved by PPP-11 than by PPP-11-Ru, giving methyl mandelate (**4a**) in 78% yield with no formation of other reduction products after 3-h irradiation. As oxidation products from TEA, diethylamine and acetaldehyde were detected. A trace of water included in methanol must contribute to their formation.

The results for photoreductions of various carbonyl compounds **2b-e** with PPP-11-Ru and PPP-11 are summarized in Table III together with their reduction potentials. It has been found that

**TABLE III: PPP-Catalyzed Photoreduction of Carbonyl Compounds with TEA<sup>a</sup>**

|   | 2                             |                               | $-E_{1/2}^{red}/V$ | PPP                 | conversion<br>of 2/% | yield <sup>c</sup> /% |           |
|---|-------------------------------|-------------------------------|--------------------|---------------------|----------------------|-----------------------|-----------|
|   | R <sup>1</sup>                | R <sup>2</sup>                |                    |                     |                      | alcohol 4             | pinacol 5 |
| a | C <sub>6</sub> H <sub>5</sub> | COOCH <sub>3</sub>            | 1.56               | PPP-11              | 98 <sup>d</sup>      | 74                    | trace     |
|   |                               |                               |                    | PPP-11-Ru           | 49 <sup>d</sup>      | 46                    | trace     |
| b | 2-pyridyl                     | H                             | 1.66               | PPP-11              | 100                  | trace                 | 35        |
|   |                               |                               |                    | PPP-11-Ru           | 66                   | trace                 | 0         |
| c | C <sub>6</sub> H <sub>5</sub> | H                             | 1.92               | PPP-11              | 87                   | trace                 | ~100      |
|   |                               |                               |                    | PPP-11-Ru           | 21                   | 6                     | 0         |
| d | C <sub>6</sub> H <sub>5</sub> | C <sub>6</sub> H <sub>5</sub> | 2.00               | PPP-11              | 97                   | 45                    | 55        |
|   |                               |                               |                    | PPP-11 <sup>e</sup> | 47                   | 57                    | 28        |
|   |                               |                               |                    | PPP-11-Ru           | trace                | 0                     | 0         |
| e | C <sub>6</sub> H <sub>5</sub> | CH <sub>3</sub>               | 2.19               | PPP-11              | 35                   | 0                     | trace     |
|   |                               |                               |                    | PPP-11-Ru           | 13                   | 0                     | trace     |

<sup>a</sup> Irradiated in methanol at >400 nm for 6 h. <sup>b</sup> Polarographic half-wave reduction potentials vs Ag/0.01 M AgNO<sub>3</sub> in methanol. <sup>c</sup> Based on **2** converted. <sup>d</sup> Irradiated for 3 h. <sup>e</sup> In CH<sub>3</sub>CN.

**Figure 8.** Photolysis of aqueous triethylamine catalyzed by PPP-11-Ru: (O) formation of diethylamine; ( $\Delta$ ) formation of ethanol; ( $\bullet$ ) H<sub>2</sub> evolution.**Figure 9.** Time-conversion plots for photoreduction of methyl benzoylformate (**2a**) to the dihydro compound **4a**: ( $\bullet$ ) catalyzed by PPP-11-Ru; ( $\circ$ ) catalyzed by PPP-11.**SCHEME I**

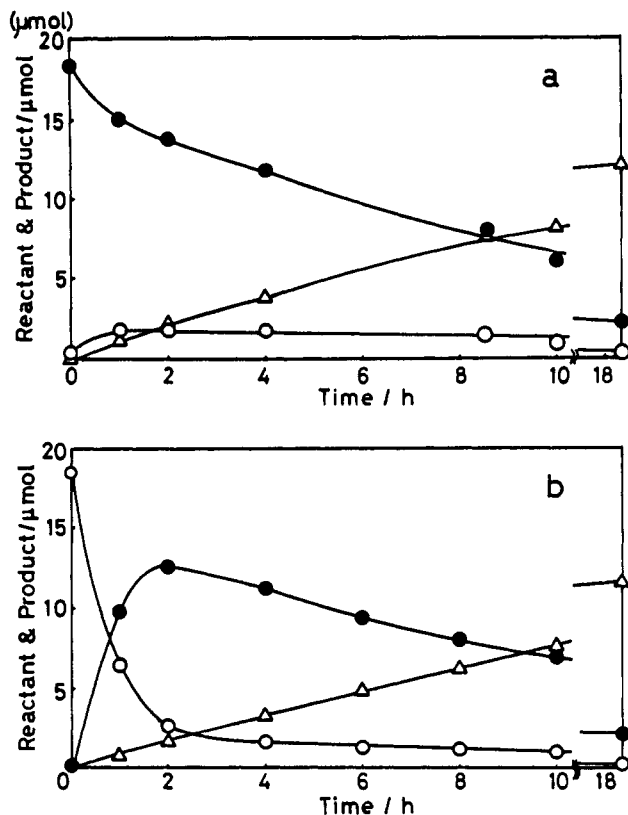
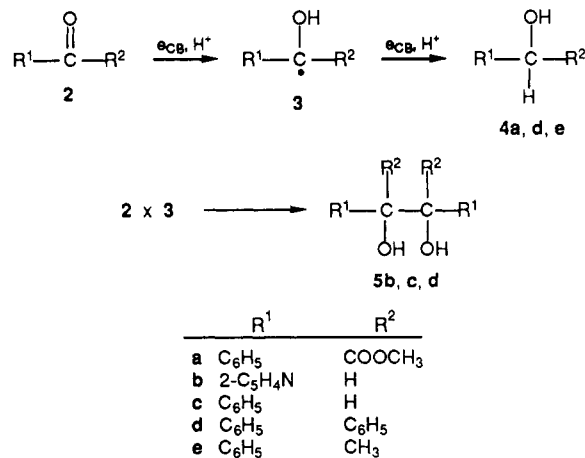


**Figure 10.** Time-conversion plots for photocatalyzed reduction of *p*-cyanocinnamitriles, **6h** (trans) and **6i** (cis), catalyzed by PPP-11 in methanol: (a) (●) disappearance of **6h**, (○) isomerization to **6i**, (Δ) reduction to the dihydro compound **9h**; (b) (○) disappearance of **6i**, (●) isomerization to **6h**, (Δ) reduction to the dihydro compound **9i**.

## SCHEME II



PPP-11 is more efficient than PPP-11-Ru in each case and the carbonyl compounds whose reduction potentials are more positive than  $-2.0$  V vs Ag/0.01 M AgNO<sub>3</sub> can be photoreduced in this system. Table III also shows that the photoreduction of **2b-d** leads to the alcohols **4b-d** as two-electron-transfer reduction products and the diols **5b-d** as dimers of the one-electron-transfer reduction intermediate **3** as shown in Scheme II.

The first one-electron-transfer reduction gives intermediary hydroxyl radical **3** after protonation, reduction potentials of which should be essential in determining the choice of the second electron-transfer or the radical-coupling reaction.<sup>23</sup> Polarographs of MBF and benzaldehyde measured in methanol indicated that MBF should undergo successive two-electron-transfer reduction at  $-1.56$  V vs Ag/0.01 M AgNO<sub>3</sub>, while benzaldehyde has the

TABLE IV: PPP-Catalyzed Photoreduction of Olefins with TEA<sup>a</sup>

|   | 6                                         |                               |                    | $-E_{red}^{b/2}$ / V | conversion of 6/% | yield <sup>c</sup> of dihydro product 9/% |
|---|-------------------------------------------|-------------------------------|--------------------|----------------------|-------------------|-------------------------------------------|
|   | R <sup>1</sup>                            | R <sup>2</sup>                |                    |                      |                   |                                           |
| f | COOCH <sub>3</sub>                        | COOCH <sub>3</sub>            | trans              | 1.80                 | 100               | 24                                        |
| g |                                           |                               | cis                | 1.84                 | 99                | 22                                        |
| h | <i>p</i> -CNC <sub>6</sub> H <sub>4</sub> | CN                            | trans              | 1.97                 | 48                | 87                                        |
| i |                                           |                               | cis                | 1.99                 | 49                | 69                                        |
| j | <i>p</i> -CNC <sub>6</sub> H <sub>4</sub> | COOCH <sub>3</sub>            | trans              | 1.97                 | 32                | 93                                        |
| k | C <sub>6</sub> H <sub>5</sub>             | COOCH <sub>3</sub>            | trans <sup>d</sup> | 2.23                 | 7                 | trace                                     |
| l |                                           |                               | cis                | 2.25                 | 26                | trace                                     |
| m | C <sub>6</sub> H <sub>5</sub>             | CN                            | trans              | 2.27                 | trace             |                                           |
| n | C <sub>6</sub> H <sub>5</sub>             | C <sub>6</sub> H <sub>5</sub> | trans              | 2.45                 | 8                 | trace                                     |
| o |                                           |                               | cis                |                      | trace             | trace                                     |

<sup>a</sup> Irradiated in methanol at  $>400$  nm for 8 h. <sup>b</sup> Polarographic half-wave reduction potentials vs Ag/0.01 M AgNO<sub>3</sub> in methanol. <sup>c</sup> Based on **6** converted. <sup>d</sup> Irradiated for 9 h.

TABLE V: Relative Intensity of Molecular Peaks in GC-Mass Spectra of Recovered Methyl *p*-Cyanocinnamate (**6j**) and the Dihydro Product (**9j**) after Photolysis

| recovered <b>6j</b>           |            | dihydro product <b>9j</b>     |            |
|-------------------------------|------------|-------------------------------|------------|
| <i>m/z</i>                    | rel intens | <i>m/z</i>                    | rel intens |
| 187 ( <i>d</i> <sub>0</sub> ) | 19.0       | 189 ( <i>d</i> <sub>0</sub> ) | 0.1        |
| 188 ( <i>d</i> <sub>1</sub> ) | 18.0       | 190 ( <i>d</i> <sub>1</sub> ) | 5.0        |
|                               |            | 191 ( <i>d</i> <sub>2</sub> ) | 6.7        |

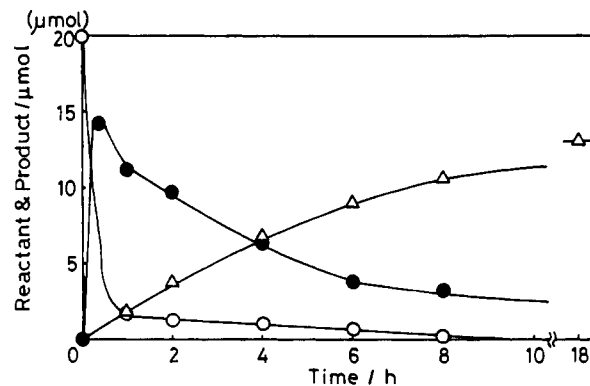


**Figure 11.** Time-conversion plots for PPP-catalyzed photoreduction of *cis*-*p*-cyanocinnamitrile (**6i**) in acetonitrile: (○) disappearance of **6i**; (●) isomerization to **6h**; (Δ) reduction to the dihydro compound **9i**.

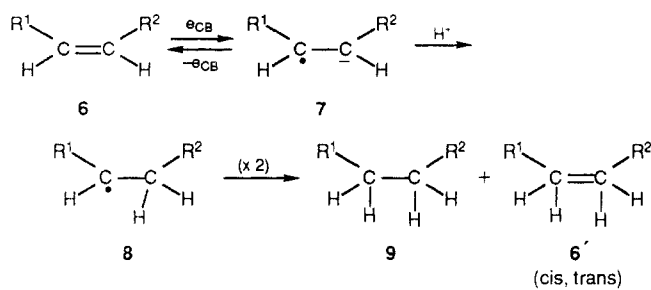
two reduction waves at  $-1.84$  and  $-1.92$  V vs Ag/0.01 M AgNO<sub>3</sub>. Because of the stepwise electron transfer to benzaldehyde, its half-reduced intermediate (**3c**) should survive at PPP interfaces. In addition, the least steric hindrance in the coupling of **3b** or **3c** should lead favorably to the formation of the diols **5b** or **5c**. As for benzophenone (**2d**), both the alcohol **4d** and the diol **5d** were formed competitively in spite of the largely negative reduction potential.

**Photoreduction of Olefins.** Parts a and b of Figure 10 show sequences of PPP-catalyzed photolysis of 4-cyanocinnamitrile (CCN) (trans, **6h**; cis, **6i**) in methanol with PPP-11 as a photocatalyst and TEA as an electron donor. Either **6h** or **6i** undergoes *cis*-*trans* photoisomerization, being sequentially photoreduced to the dihydro compound (**9h**) in good yield. Table IV presents the results of photoreduction of other olefins **6** whose reduction potentials range from  $-1.80$  to  $-2.45$  V vs Ag/0.01 M AgNO<sub>3</sub>. Apparently, the photoreduction of the carbon-carbon double bond can be readily accomplished by the PPP photosystem when their reduction potentials are more positive than  $-2.0$  V vs Ag/0.01 M AgNO<sub>3</sub>. Interestingly, although the reduction potential of olefins (**6f-j**) is comparable to that of benzaldehyde (**2c**), they underwent the exclusive two-electron-transfer photoreduction, yielding dihydro compounds (**9f-j**) in fair to good yields.

The isomerization and reduction of CCN have been found to proceed much more quickly in acetonitrile than in methanol as shown in Figure 11; **6i** isomerized to **6h** very rapidly, and **6h** was photoreduced to **9h** in better yield. After reaching a photo-stationary state of the isomerization, the apparent quantum yields

(23) Ishitani, O.; Yanagida, S.; Takamuku, T.; Pac, C. *J. Org. Chem.* **1987**, *52*, 2790.

## SCHEME III



|   | R <sup>1</sup>                            | R <sup>2</sup>             |   | R <sup>1</sup>                | R <sup>2</sup>                        |
|---|-------------------------------------------|----------------------------|---|-------------------------------|---------------------------------------|
| f | COOCH <sub>3</sub>                        | COOCH <sub>3</sub> (trans) | k | C <sub>6</sub> H <sub>5</sub> | COOCH <sub>3</sub> (trans)            |
| g | COOCH <sub>3</sub>                        | COOCH <sub>3</sub> (cis)   | l | C <sub>6</sub> H <sub>5</sub> | COOCH <sub>3</sub> (cis)              |
| h | <i>p</i> -CNC <sub>6</sub> H <sub>4</sub> | CN (trans)                 | m | C <sub>6</sub> H <sub>5</sub> | CN (trans)                            |
| i | <i>p</i> -CNC <sub>6</sub> H <sub>4</sub> | CN (cis)                   | n | C <sub>6</sub> H <sub>5</sub> | C <sub>6</sub> H <sub>5</sub> (trans) |
| j | <i>p</i> -CNC <sub>6</sub> H <sub>4</sub> | COOCH <sub>3</sub> (trans) | o | C <sub>6</sub> H <sub>5</sub> | C <sub>6</sub> H <sub>5</sub> (cis)   |

for the disappearance of **6h** and the dihydro product (**9h**) were determined to be 0.058 and 0.039 at 405 nm, respectively.

In order to clarify the mechanism of the eventual two-electron-transfer photoreduction and its relationship with the photoisomerization, the photolysis of methyl 4-cyanocinnamate **6j** was carried out in methanol-*O-d* at a 50% conversion. The unreacted **6j** and the dihydro product **9j** were analyzed by GC-mass spectroscopy. In Table V are summarized the relative intensities of molecular ion peaks of the reactant and product. It has been found that about 50% of the recovered **6j** was monodeuterated, whereas the product **9j** was a 1:1 mixture of the monodeuterated and the dideuterated compounds. These results strongly suggest that the photoreduction and photoisomerization should proceed to give one-electron-transfer reduction intermediates, **7** and **8**, and that the disproportionation of **8** should eventually give the two-electron-transfer reduction products **9** as shown in Scheme III.

## Discussion

It is striking that, under visible-light irradiation, organic compounds whose reduction potentials are more positive than  $-2.00$  V vs Ag/0.01 M AgNO<sub>3</sub> are photoreducible by photooxidizing amines whose oxidation potentials are around 1.0 V vs Ag/0.01 M AgNO<sub>3</sub>. High surface areas and good dispersion due to low densities should also be convenient for the heterogeneous photocatalysis.

Since the discovery of the high conductivity of doped PPP,<sup>24</sup> several papers have been published on the electronic structure of oligo(*p*-phenylene) and PPP.<sup>11,25,26</sup> Theoretical studies revealed that the band gap in the series of *p*-phenyls does not change so much with increasing phenylene units as that in the series of the acenes and that the band gap has a tendency to level off around 3.2 eV.<sup>27</sup> In fact, in the photoacoustic spectra, the shift to the longer wavelength levels off with increasing phenylene units and the band gap of both PPP-7 and PPP-11 was determined to be 2.90 eV, although PPP-11 should include much longer *p*-phenylene chains than PPP-7 (Figure 2b).

Contrary to our expectation, the IP of PPP in the solid state was found to increase with increasing *p*-phenylene chains. The theoretical IP values were determined, depending on the geometry of *p*-phenylene chains,<sup>11a</sup> to be 5.5 or 5.65<sup>11c</sup> eV for the coplanar, 5.6 eV for the twisted (22°), and 6.9 eV for the perpendicular structures. Accordingly, the IP value of solid PPP-11 determined

by AUP is about 0.5 eV larger than the theoretically predicted value for the coplanar geometry.<sup>11</sup> However, the energy structure of PPP photocatalysts derived from the observed IP is quite consistent with the photocatalytic results (Table I); the threshold of photoredox reactions on PPP-11 agrees well with the band structure of PPP-11. On the other hand, the slow H<sub>2</sub> evolution for the PPP-7-catalyzed water photoreduction can be explained as due to the less positive valence band potential, i.e., the poorer oxidizing power of PPP-7 compared to PPP-11. In addition, because of inverted region effects,<sup>28</sup> the larger energy gap between the conduction band and the reduction potential of the proton ( $E^{\text{red}} = -0.58$  V vs Ag/0.01 M AgNO<sub>3</sub>) might also be responsible for the slow H<sub>2</sub> evolution in the PPP-7 system.

With regard to the effect of noble metals on PPP-photocatalyzed water reduction, metals under specific interaction with PPP molecules should mediate electrons from the conduction band to water. In line with the inverted region effects,<sup>28</sup> the potent conduction band electrons should be kinetically favorable for the electron transfer to organic compounds having appropriate reduction potential, and metal relays may work well for the reduction of water as reported for inorganic semiconductor photocatalysts.<sup>2,29b</sup>

In the photocatalysis of PPP, some solvent effects were observed. During water photoreduction, ethanol was formed through the photoreduction of acetaldehyde. However, 2,3-butanediol, a coupling product of a one-electron-transfer reduction intermediate from acetaldehyde, was not detected. This fact contrasts dramatically with the photoreduction of aldehydes in nonaqueous medium. Presumably, protic circumstance may affect the course of the reduction. In addition, an enhanced rate of photoreduction was observed in acetonitrile, suggesting that a polar solvent should contribute to the stabilization of intermediary one-electron-transfer intermediates or the charge-separated states of the PPP assembly. In dried aprotic solvents such as benzene and THF, however, neither the photoreduction nor the photoisomerization of CCN could be observed. This failure was ascribed to the complete absence of a proton source in the reaction system.

The disproportionation mechanism plays an important role in the present photoreduction of carbonyls and olefins. The photoreduction of **2d** was carried out in acetonitrile, and the exclusive formation of the coupling product **5d** (See Table II) was expected because of the absence of protons that could inhibit the ECE process (electron-proton-electron transfer) that should lead exclusively to alcohols **4**.<sup>23</sup> However, the alcohol **5d** was formed to the same extent as in methanol, possibly through an effective disproportionation reaction of the half-reduced intermediate **3d**. The formation of **3d** may be assisted by a trace of water present in acetonitrile.

The cis-trans photoisomerization occurred much more quickly than the photoisomerization of 2-octene that we reported previously.<sup>14</sup> Further, it was confirmed that TEA is indispensable for the present photoisomerization but the photoisomerization of 2-octene occurs either in the presence or absence of TEA. Thus, the present photoisomerization should proceed through the back electron transfer from **7** (Scheme III), which mechanism is quite different from that of the previously reported photoisomerization.<sup>14</sup>

There are some aspects indicating an abnormality in the photocatalysis and properties of PPP as follows: (1) only photodeposited noble metals show the characteristic enhancement of the water photoreductive H<sub>2</sub> evolution; (2) one-electron-transfer reductions are prevailing in the PPP photocatalysis, leading to the coupling, disproportionation, and isomerization reactions;<sup>29</sup> (3)

(24) (a) Ivory, D. M.; Miller, G. G.; Sowa, J. M.; Shacklette, L. W.; Chance, R. R.; Baughman, R. H. *J. Chem. Phys.* **1979**, *71*, 1506. (b) Shacklette, L. W.; Chance, R. R.; Ivory, D. M.; Miller, G. G. *Synth. Met.* **1979**, *1*, 307. (c) Baughman, R. H.; Shacklette, L. W.; Eckhardt, H.; Chance, R. R.; Miller, G. G.; Ivory, D. M.; Baughman, R. H. *J. Chem. Phys.* **1980**, *73*, 4098.

(25) Duke, C. B.; Paton, A. In *Conductive Polymers*; Seymour, R. B., Ed.; Plenum Press: New York, 1981; p 155.

(26) The experimental IP value (5.3 eV) of PPP was previously obtained from its oxidation potential on the basis of their linear relationship. However, the details of the experiments are unpublished. See ref 11b.

(27) Riga, J.; Pireaux, J. J.; Boutique, J. P.; Caudano, R.; Verbist, J. J.; Gobillon, Y. *Synth. Met.* **1981**, *4*, 99.

(28) Miller, J. R.; *Nouv. J. Chem.* **1987**, *11*, 83, and references cited therein.

(29) In our group, sequential two-electron-transfer reductions were observed in ZnS-catalyzed photolyses of primary amines or aldehydes. During the photolyses, photoreductions of intermediary Schiff bases and aldehydes occurred efficiently in water, giving respective secondary amines and alcohols without much H<sub>2</sub> evolution, which was ascribed to the large energy gap between the conduction band level of ZnS and the reduction potential of water. (a) Yanagida, S.; Kizumoto, H.; Ishimaru, Y.; Pac, C.; Sakurai, H. *Chem. Lett.* **1985**, 141. (b) Yanagida, S.; Ishimaru, Y.; Miyake, Y.; Shiragami, T.; Pac, C.; Hashimoto, K.; Sakata, T. *J. Phys. Chem.* **1989**, *93*, 2576.

the action spectrum for the water photoreduction has a maximum around the band gap (405 nm), and the shorter wavelength UV light was not effective for the photoreduction; (4) the observed leveling off of the band gaps of the PPP's supports the existence of  $\pi$ -electronic interactions in PPP, but they are weak compared with the acenes;<sup>26</sup> (5) PPP's have fairly low densities, although they include heavy bromine atoms; and (6) PPP's have unexpectedly large ionization potentials, although the  $\pi$ -conjugation should exist to some extent.

It is well-known that planar molecules have fairly high densities because they can be packed together well and the addition of heavy atoms increases the density; also the densities are lowered by loose and irregular packing of the molecules.<sup>30</sup> Thus, the low densities of PPP's suggest that the *p*-phenylene chains should be packed loosely because of the decreased planarity of the chains. Further, the nonplanar and largely twisted *p*-phenylene units on the external parts of solid PPP's might be responsible for the large IP values. These observations and rationalizations seem to suggest a contribution of electrons existing in exciton states rather than from completely free electrons in the conduction band.

### Conclusion

This is the first observation of visible-light-driven interfacial charge separation and the concomitant electron- and hole-transfer processes on  $\pi$ -conjugated polymers. The solid-state characteristics of the PPP photocatalysts were elucidated by spectroscopic analysis, by photolysis of a series of different electron acceptors and donors, and by AUP analysis. The energetic structure thus obtained was in good agreement with the threshold observed in the photocatalysis. It was also shown that hydrophobic PPP surfaces should organize well the accompanying thermal reactions occurring after the photochemical charge separation. Taking into account the unusual photocatalytic and related properties of solid PPP, the effective photocatalysis could be ascribed to a photochemical change of conformation of surface *p*-phenylene units, i.e., negatively and positively charged quinoidlike structures of *p*-phenylene chains.

### Experimental Section

**Materials.** 1,4-Dibromobenzene, 4,4'-dibromobiphenyl, RuCl<sub>3</sub>, RhCl<sub>3</sub>, PdCl<sub>2</sub>, K<sub>2</sub>PtCl<sub>6</sub>, *p*-terphenyl, and *p*-sexiphenyl were extra-pure (EP) grade from Tokyo Kasei and were used without further purification. Platinum black was obtained from Japan Engerhart. *n*-Butylamine, diethylamine, dimethylamine, di-*n*-propylamine, triethylamine, trimethylamine, tri-*n*-propylamine, *N,N*-dimethylbenzylamine (DBM), *N,N*-dimethyltoluidine (DMT), *tert*-butylamine, benzylamine, ascorbic acid, EDTA Na salt, dimethyl fumarate (**6f**), dimethyl maleate (**6g**), *trans*-methyl cinnamate (**5k**), *trans*-cinnamitrile (**6m**), stilbene (**6n,o**), and methanol-*O-d* were obtained as EP grade from Nakalai Tesque. Hydrazine hydrate was EP grade from Wako Pure Chemicals. The carbonyl compounds (**2a-e**) were obtained from Nakalai Tesque and purified by recrystallization or distillation. Triethylamine, diethylamine, and DMT were distilled under argon atmosphere before use. Methanol was distilled in the presence of magnesium methoxide. Water was deionized and distilled with potassium permanganate.

NiCl<sub>2</sub>(bpy) was prepared from NiCl<sub>2</sub> and 2,2'-dipyridyl according to the reported procedure.<sup>31</sup> Methyl cinnamate (cis, **6l**) was obtained by photoisomerization of **6k** in benzene and purified by column chromatography. *p*-Cyanocinnamitriles (**6h,i**) were obtained from *p*-cyanobenzaldehyde and cyanoacetic acid, and the isomers were separated by column chromatography.<sup>32</sup> Methyl *p*-cyanocinnamate (trans, **6j**) was prepared by the esterification of the cinnamic acid obtained from *p*-cyanobenzaldehyde and malonic acid.<sup>33</sup>

**Analysis.** H<sub>2</sub> evolution was analyzed by GLC using an activated carbon column (2 m × 3 mm) on a Shimadzu Model GC-3BT at 100 °C. Product analysis was carried out by GLC using a Shimadzu Model GC-7AF apparatus equipped with a flame ionization detector and the following columns: a 3-m × 3-mm column of ASC-L for diethylamine and ethanol; a 1- or 2-m × 3-mm column of UCON LB550X for methyl benzoylformate, benzophenone, 2-pyridinealdehyde; a 1-m × 3-mm column of PEG 20M for *p*-cyanobenzaldehyde and benzaldehyde; a 0.5-m × 3-mm column of OV-1 for the pinacol from benzaldehyde.

GC-mass analysis was conducted on a JEOL Model JMS-DX300 using a 1-m × 3-mm column of OV-17 (3%).

UV spectra were recorded on a Hitachi Model 220A spectrophotometer and a Photal (Otsuka Electronics) with a spectromultichannel photodetector (Model MCPD-100). Steady-state photoluminescence spectra were recorded on a Hitachi Model 850 spectrometer. X-ray microanalysis (XMA) was carried out using a Hitachi Model EPMA X-650.

Micrographs were obtained with a scanning electron microscope apparatus, Hitachi Model S-800. The specific surface area of PPP powders was determined by the volumetric BET method with a Shimadzu Model 2205-Ar apparatus using argon as adsorbent.

Polarographic measurements were performed for air-free dry solutions containing **2a-e** or **6f-o** and a supporting electrolyte (0.1 M), sodium perchlorate in methanol or tetraethylammonium perchlorate in acetonitrile, at 20 ± 0.1 °C by using a Yanagimoto Model P-1100 potentiostat. The reference electrode is an Ag/0.01 M AgNO<sub>3</sub> in methanol or acetonitrile, and the working electrode was a dropping Hg electrode at a 67-cm pressure operated at a pulse-regulated dropping time of 0.5 s.

Ionization potential was determined by an atmospheric ultraviolet photoelectron (AUP) analyzer Model AC-1 (Riken Keiki Co., Ltd.). In the AUP measurements, a beam of monochromatic light of energy  $h\nu$  (3–6 eV) impinges upon the sample surface and excites valence band electrons to vacuum level. Low-energy electrons emitted from a solid surface in the air are counted by means of an air counter for determination of the threshold energy for electron emission. The ionization potential was deduced to correspond to the upper edge of the valence band of the substrate. The electrochemical position of the valence level,  $E_v$  (V vs Ag/0.01 M AgNO<sub>3</sub>) was calculated from  $E_v = IP - 5.04$ .<sup>11b,34</sup>

Quantum yields were determined by using potassium ferrioxalate as an actinometer. The incident light was isolated from a xenon lamp by using a Hitachi Model MPF-2A monochromator ( $1.63 \times 10^{15}$  quanta/s).

**Synthesis of PPP.** PPP was synthesized by Yamamoto's method<sup>15</sup> as follows. Ni(bpy)Cl<sub>2</sub> was employed as a polymerization catalyst. PPP-7 was prepared by polymerization of the Grignard reagent obtained from 4,4'-dibromobiphenyl and magnesium (mole ratio, 1:1) in THF. As for PPP-11, 1,4-dibromobenzene was used instead of 4,4'-dibromobiphenyl. The resulting polymers were washed thoroughly with ethanol, aqueous HCl, and THF, extracted by toluene with a Soxhlet apparatus and dried without heating. Anal. Found for PPP-7: C, 79.30; H, 4.89; Br, 14.14. Anal. Found for PPP-11: C, 84.86; H, 5.05; Br, 8.37.

According to Kovacic's method,<sup>20</sup> dark-brown PPP powder was also prepared by polymerization of benzene with AlCl<sub>3</sub> and CuCl<sub>2</sub>. The IR spectrum was identical with PPP-7 and PPP-11.

**Photodeposition of Metal on PPP.** A typical example is as follows:<sup>35</sup> PPP-11 (100 mg) and RuCl<sub>3</sub> (5 mg) were placed in a Pyrex tube containing TEA (5 mL), water (5 mL), and ethanol (5 mL). The PPP suspended solution was stirred magnetically and irradiated for 3 h with 700-W Hg arc lamp. The supernatant solution was bleached as the reaction proceeded. The resulting suspension was filtered off, washed with methanol, and dried in vacuo. XMA analysis revealed that Ru (1.4%) was deposited homogeneously. However, ESCA analysis of PPP-11-Ru using a Shimadzu electron spectrometer Model ESCA 750 was un-

(30) Stout, G. H.; Jensen, L. H. *X-ray Structure Determination*; Macmillan: London, 1968; p 80.

(31) Broomhead, J. A.; Dwyer, F. P. *Aust. J. Chem.* **1961**, *14*, 250.

(32) Pac, C.; Miyauchi, Y.; Ishitani, O.; Ihama, M.; Yasuda, M.; Sakurai, H. *J. Org. Chem.* **1984**, *49*, 26.

(33) Davies, W.; Holmes, B. M. *J. Chem. Soc.* **1939**, 357.

(34) For conversion to Ag/AgNO<sub>3</sub> basis, see: Bard, A. J., Ed. *Electroanalytical Chemistry*; Dekker: New York, 1969; Vol. 3, p 57.

(35) Krautler, B.; Bard, A. J. *J. Am. Chem. Soc.* **1978**, *100*, 2239.

successful because of the low content.

Rhodium, platinum, and palladium were similarly photodeposited on PPP-11 from  $\text{RhCl}_3$ ,  $\text{K}_2\text{PtCl}_6$ , and  $\text{PdCl}_2$ , respectively.

**Water Photoreduction.** To a mixture of methanol, water, and TEA (each 0.5 mL) in a Pyrex tube (8 mm in diameter) was added PPP or metal-loaded PPP (10 mg). The resulting suspension was flashed with argon gas under cooling on an ice bath, closed off with a gum stopper, and irradiated with stirring at room temperature (25 °C) by >400- or >290-nm light. The inner gas was analyzed by GLC.

**Photoreduction of Organic Substrates.** To 2 mL of methanolic TEA (1 M) and PPP (10 mg) solution in a Pyrex tube (8 mm in diameter) was added a substrate in an amount to make a 1 mM solution for carbonyl compounds and 10 mM solution for olefins. The resulting PPP-suspended solution was flashed with argon gas under cooling on an ice bath and then irradiated at 25 °C with a 500-W halogen lamp fitted with a sodium nitrite solution filter. Stirring was accomplished by using a magnetic stir bar (5 mm  $\times$  2 mm). The products analysis was performed by periodic GLC or HPLC analysis. It was confirmed that no reaction occurs in the dark or in the absence of PPP.

**Determination of Deuterium Isotopic Distribution.** Photoreduction of methyl 4-cyanocinnamate (trans, **6j**) was performed in methanol-*O-d* as mentioned above. When a half-amount of

the substrate disappeared, the irradiation was stopped, the reaction suspension was filtered off, and the filtrate was evaporated. The residue was analyzed by GC-mass spectroscopy, and the relative intensity was compared as summarized in Table V.

**Acknowledgment.** We thank Professor K. Yoshino at Osaka University and Dr. A. Nozik at SERI for helpful comments and suggestions. We also thank Professor M. Yokoyama (E. Miyamoto from Mita Industries, Ltd.), Professor H. Nagai, Dr. M. Matsumura, and Dr. M. Hiramoto at Osaka University for their kind measurements of respective AUP, XMA, ESCA, and micrographs. This work was supported by the Iwatani Naoki Foundation's Research Grant and the General Sekiyu Research and Development Encouragement and Assistance Foundation and by a Grant-in-aid for scientific Research from the Ministry of Education, Science and Culture, Japan (Nos. 61040003 and 62213021).

**Registry No.** **2a**, 15206-55-0; **2b**, 1121-60-4; **2c**, 100-52-7; **2d**, 119-61-9; **2e**, 98-86-2; **6f**, 624-49-7; **6g**, 1587-15-1; **6h**, 27519-25-1; **6i**, 79430-98-1; **6j**, 67472-79-1; **6k**, 1754-62-7; **6l**, 19713-73-6; **6m**, 1885-38-7; **6n**, 103-30-0; **6o**, 645-49-8; PPP, 25190-62-9; Ru, 7440-18-8;  $\text{H}_2\text{O}$ , 7732-18-5;  $\text{H}_2\text{NNH}_2$ , 302-01-2;  $\text{Et}_3\text{N}$ , 121-44-8;  $\text{NPr}_3$ , 102-69-2;  $\text{NMe}_3$ , 75-50-3;  $\text{HNPr}_2$ , 142-84-7;  $\text{HNEt}_2$ , 109-89-7;  $\text{HNMe}_2$ , 124-40-3;  $\text{H}_2\text{N-Pr}$ , 107-10-8;  $\text{H}_2\text{NBu}$ , 109-73-9;  $\text{H}_2\text{NCH}_2\text{Ph}$ , 100-46-9;  $\text{NH}_3$ , 7664-41-7;  $\text{H}_2\text{NBu-t}$ , 75-64-9.

## Low-Energy Electron Diffraction and Voltammetry of Carbon Monoxide Electrosorbed on Pt(111)

D. Zurawski, M. Wasberg, and A. Wieckowski\*

Department of Chemistry, School of Chemical Sciences, University of Illinois, Urbana, Illinois 61801  
(Received: August 10, 1989)

The organization of carbon monoxide electrosorbed at various coverages on a Pt(111) single-crystal electrode has been studied by using ex situ characterization by low-energy electron diffraction. Two CO structures, ( $\sqrt{3} \times \sqrt{3}$ )rect and  $c(\sqrt{3} \times \sqrt{5})$ rect, have been identified for saturation and partial coverage, respectively. A third structure,  $c(4 \times 2)$ , was observed after prolonged exposure of a saturation coverage of CO to the UHV environment. The packing density of electrosorbed CO attained at saturation coverage is higher than that observed in gas-phase research for CO adsorbed at room temperature; however, it is comparable with the maximum coverage attained for low-temperature gas-phase adsorption. The appearance of the  $c(\sqrt{3} \times \sqrt{5})$ rect structure at all partial coverages of electrosorbed CO has been interpreted as being indicative of the formation of islands of this high-coverage structure in the electrochemical environment. Current-potential profiles obtained for partial coverages exhibit two distinguishable peaks which have been attributed to the oxidation of CO adsorbed in different sites within the adlattice. Through a correlation of the voltammetric results, the organizational information obtained from LEED measurements, and structures proposed by gas-phase researchers, the two current peaks have been assigned to CO adsorbed in  $c(4 \times 2)$  domains and in high-density fault lines bordering these domains.

### Introduction

Carbon monoxide is a template molecule in gas-phase surface science investigations. Its molecular simplicity and high absorbance of infrared radiation and practical considerations regarding its poisonous properties toward most catalytic surfaces make this molecule an ideal object for such research. The accumulated molecular-level information on this particular system has contributed significantly to the understanding of two-dimensional chemistry<sup>1</sup> and heterogeneous catalysis,<sup>2</sup> and in the area of molecular structures coordinated to metal atoms and metal cations.<sup>3,4</sup>

Until recently, the lack of proper research tools has prevented surface electrochemists from acquiring proper insight into the matter on the level easily accessible in gas-phase surface science. The development of several new methodologies is rapidly changing the scope and depth of "liquid-phase" surface science. In particular, a successful combination of ultrahigh vacuum (UHV) and electrochemical techniques<sup>5</sup> and in situ vibrational analysis of the liquid-solid adsorbates<sup>6</sup> are instrumental in documenting the nature of adsorbates such as carbon monoxide. Using one or both of these approaches enables researchers to characterize the chosen liquid-solid interfacial objects and compare them with the analogue systems created under gas-phase conditions. The goal of this work is to present such a comparison in the case of the

(1) Somorjai, G. A. *Chemistry In Two Dimensions: Surfaces*; Cornell University: New York, 1981; pp 185-187.

(2) Goodman, D. W. *Acc. Chem. Res.* **1984**, *17*, 194.

(3) Bagus, P. S.; Hermann, K.; Bauschlicher, C. W. Jr. *J. Chem. Phys.* **1984**, *81*(4), 1966.

(4) Ertl, G. In *The Nature of the Surface Chemical Bond*; Rhodin, T. N., Ertl, G., Eds.; North-Holland: Amsterdam, 1978; Chapter 5.

(5) Hubbard, A. T. *Acc. Chem. Res.* **1980**, *13*, 177.

(6) Bewick, A.; Pons, S. In *Advances in Infrared and Raman Spectroscopy*; Clark, R. J. H., Hester, R. E., Eds.; Wiley Heyden: New York, 1985; Vol. 12, Chapter 1.